Fusion Channels of Non-Abelian Anyons from Angular-Momentum and Density-Profile Measurements

E. Macaluso,[1] T. Comparin,[1] L. Mazza,[2] and I. Carusotto[1]
[1]INO-CNR BEC Center and Dipartimento di Fisica, Università di Trento, 38123 Trento, Italy
[2]LPTMS, CNRS, Université Paris-Sud, Université Paris-Saclay, 91405 Orsay, France

(Received 1 April 2019; published 26 December 2019)

We present a method to characterize non-Abelian anyons that is based only on static measurements and that does not rely on any form of interference. For geometries where the anyonic statistics can be revealed by rigid rotations of the anyons, we link this property to the angular momentum of the initial state. We test our method on the paradigmatic example of the Moore-Read state that is known to support excitations with non-Abelian statistics of Ising type. As an example, we reveal the presence of different fusion channels for two such excitations, a defining feature of non-Abelian anyons. This is obtained by measuring density-profile properties, like the mean square radius of the system or the depletion generated by the anyons. Our study paves the way to novel methods for characterizing non-Abelian anyons, both in the experimental and theoretical domains.

DOI: 10.1103/PhysRevLett.123.266801

Introduction.—The standard classification of particles into bosons and fermions breaks down in two spatial dimensions, where exotic objects known as anyons can exist [1–6]. The key concepts for defining the statistics of anyons are the adiabatic motion of one anyon around another, hereafter the braiding, and the adiabatic exchange of the anyons positions [7]. Anyons can be characterized by merging two of them, and the properties of the new composite object depend on the fusion rules of the original anyons. When there is the possibility of fusing in more than one way, anyons can be non-Abelian [8–11]: they are the heart of topological quantum computation [12], and their experimental realization is thus highly desired. Several existing platforms are expected to host them as emergent quasiparticles, but the unambiguous experimental demonstration of their properties is still the matter of an intense debate [13,14].

In the last twenty years, several works addressed the problem of extracting the properties of the anyons hosted by the ground states of a given Hamiltonian. The simplest approach relies on explicitly following the ground-state evolution when anyons are exchanged [15–19]. Within other approaches, the analytical study of paradigmatic wave functions has also clarified important issues about the statistics of excitations [10,20,21]. On the experimental side, interferometric schemes have been proposed to compare the state before and after the adiabatic time evolution [15,22–26], but none of them has produced unambiguous results [27,28].

We propose a method to characterize non-Abelian anyons: By considering geometries where the anyonic statistics can be revealed through rigid rotations of the anyons (see Fig. 1), we relate their statistical phase to the angular momentum and to the density profile of the system. This protocol allows one to identify the existence of different fusion channels, a defining property of non-Abelian anyons, with remarkable experimental simplicity in the context of ultracold atoms [29,30] and photons [31,32]. Moreover, our study represents a powerful theoretical tool to inspect excitations with unknown statistics, going beyond the observation of multiple fusion channels. As a showcase study, we discuss our method for the case of the Moore-Read (MR) state [8], and outline an experimental procedure for computing the statistical phases of its quasiholes.

Rigid rotations of the anyons.—We consider a two-dimensional (2D) system of N particles (bosons or fermions) supporting anyonic excitations. The Hamiltonian $\hat{H}_1$ is a function of particle positions and momenta, as well as of time. We use the complex coordinate notation $z_j = x_j + iy_j$ for the position of the jth particle. The time dependence of $\hat{H}_1(\partial_{z_j}, \partial_{\bar{z}_j}, z_j, \bar{z}_j; t)$ is only due to a set of parameters $\eta_\mu(t)$ defining the centers of some external local potentials $V_{\text{ext}}(z, \eta_\mu(t))$. These potentials typically couple

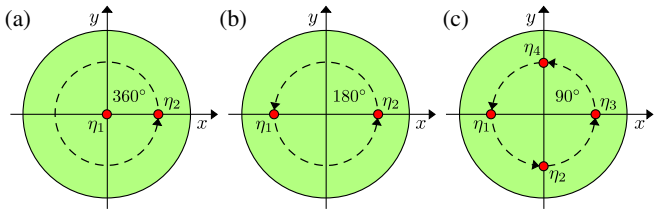

FIG. 1. [(a)–(c)] Rigid rotations of two anyons [panels (a) and (b)] or four anyons [panels (c)]. Rotation angles are such that the set of anyonic coordinates (red dots) remains the same.

with the particle density, creating and pinning the anyons at positions $\eta_\mu(t)$ [15,33–36].

To reveal the anyonic statistics, one option is to braid the anyons through rigid rotations of the pinning-potential coordinates (see Fig. 1). These transformations are defined as

$$\eta_\mu(t) = \eta_\mu(0)e^{i\theta(t)}, \qquad \theta(t) = \frac{t}{T}\theta_f, \tag{1}$$

where θ_f is the final rotation angle and T is the time duration of the process.

Since we consider rigid rotations, we can study the problem in the reference frame R_2 corotating with the anyons, rather than using the laboratory reference frame R_1. We assume that $V_{\text{ext}}(z, \eta_\mu(t))$ is a function of the distance $|z - \eta_\mu(t)|$ between particles and anyons, and that the remaining terms in $\hat{H}_1$ are rotationally invariant. Under these assumptions, the generator of the time evolution in R_2 in the time span $[0,T]$ reads [29]

$$\hat{H}_2(\partial_{z_j}, \partial_{\bar{z}_j}, z_j, \bar{z}_j; t) = \hat{H}_1(\partial_{z_j}, \partial_{\bar{z}_j}, z_j, \bar{z}_j; t = 0) - \frac{\theta_f}{T}\hat{L}_z, \tag{2}$$

which is manifestly time independent. The first term on the right-hand side is the initial Hamiltonian in R_1, while the second one describes the effect of the rotation. Being interested in an adiabatic process, we consider $T \to \infty$. The rotation term is then a small contribution and can be treated perturbatively.

To describe the dynamics in R_2, we consider an initial state $|\Psi_0\rangle$ belonging to the m-fold degenerate ground-state manifold $\mathcal{H}_{E_0}$, spanned by the basis $\{|\psi_\alpha\rangle\}_{\alpha=1,\ldots,m}$, with $\hat{H}_1(t=0)|\psi_\alpha\rangle = E_0|\psi_\alpha\rangle$ and $\langle\psi_\alpha|\psi_\beta\rangle = \delta_{\alpha\beta}$. If the dynamics is slow enough, we can use the adiabatic theorem to state that the dynamics is restricted to $\mathcal{H}_{E_0}$ (an explicit proof is in [37]), and make the following ansatz:

$$|\Psi_2(t)\rangle = e^{-iE_0 t/\hbar}\sum_{\alpha=1}^{m}\gamma_\alpha(t)|\psi_\alpha\rangle, \quad \gamma_\alpha(0) = \langle\psi_\alpha|\Psi_0\rangle. \tag{3}$$

By applying the Schrödinger equation, we recover the time-evolution equation of the γ_α's,

$$i\hbar\frac{d\gamma_\alpha(t)}{dt} = -\frac{\theta_f}{T}\sum_{\beta=1}^{m}\mathcal{L}_{\alpha\beta}\gamma_\beta(t), \tag{4}$$

where $\mathcal{L}_{\alpha\beta} = \langle\psi_\alpha|\hat{L}_z|\psi_\beta\rangle$ is the angular momentum restricted to $\mathcal{H}_{E_0}$. The solution reads

$$|\Psi_2(T)\rangle = e^{-i\hat{H}_2 T/\hbar}|\Psi_0\rangle = e^{-iE_0 T/\hbar}e^{i\theta_f\mathcal{L}/\hbar}|\Psi_0\rangle, \tag{5}$$

in terms of the matrix exponential $\exp[i\theta_f\mathcal{L}/\hbar]$.

To find the state $|\Psi_1(T)\rangle$ in the laboratory frame, we need to rotate $|\Psi_2(T)\rangle$ by an angle θ_f,

$$\begin{aligned}|\Psi_1(T)\rangle &= e^{-i\theta_f\hat{L}_z/\hbar}|\Psi_2(T)\rangle \\ &= e^{-iE_0T/\hbar}e^{-i\theta_f\hat{L}_z/\hbar}e^{i\theta_f\mathcal{L}/\hbar}|\Psi_0\rangle.\end{aligned} \tag{6}$$

The state in Eq. (6) is the exact result for an adiabatic braiding process performed through a rigid rotation of all anyons by an angle θ_f. We recognize a dynamical phase proportional to T that is unessential to the discussion of non-Abelian statistics and therefore neglected from now on. The remaining geometric contribution is the product of two unitary matrices: $\mathcal{B}$, with matrix elements $\mathcal{B}_{\alpha\beta} = \langle\psi_\alpha|e^{-i\theta_f\hat{L}_z/\hbar}|\psi_\beta\rangle$, and $\mathcal{U}_B \equiv e^{i\theta_f\mathcal{L}/\hbar}$, which is the Berry matrix of the adiabatic process under study, once one makes a suitable choice of the basis states for each angle $\theta(t)$ [37].

To guarantee that the ground-state manifold is $\mathcal{H}_{E_0}$ at both times [12], the angle θ_f must be such that $\hat{H}_1(t)$ is the same at times $t = 0$ and T. Depending on the anyon positions, this constraint can be satisfied even for rotation angles that are not multiples of 2π [see Figs. 1(b)–1(c)]. When $\theta_f = 2\pi k$, with k integer, $\mathcal{B}$ is trivially the identity matrix. In this case, $\mathcal{U}_B$ encodes the full geometrical contribution to the time evolution, made up of both topological and nontopological parts. We stress that $\mathcal{U}_B$ only depends on measurable properties of the ground-state manifold at the initial time, namely, the angular-momentum matrix elements. Therefore, no actual time evolution is needed to measure it, which constitutes an undeniable experimental advantage. The case of $\theta_f \neq 2\pi k$ is relevant in the theoretical context, where—in contrast with experimental studies—nothing precludes the extraction of $\mathcal{B}$ (see an example in Ref. [37]). A comprehensive analysis of this case is left for a future work.

Moore-Read state and its quasihole excitations.—We now consider the MR state, which is described by the wave function [8]

$$\Psi(\{z_j\}) = \text{Pf}(W)\prod_{i<j}(z_i - z_j)^M e^{-\sum_i |z_i|^2/4l_B^2}, \tag{7}$$

where l_B is the magnetic length. $\text{Pf}(W)$ denotes the Pfaffian of the $N \times N$ antisymmetric matrix W, with $W_{ij} = 1/(z_i - z_j)$ for $i \neq j$. For even (odd) values of the positive integer M, this wave function represents a fermionic (bosonic) fractional quantum hall (FQH) state at filling $\nu = 1/M$, which belongs to the lowest Landau level (LLL) [7]. This state is the ground state for 2D charged particles, in the presence of a transverse magnetic field and of a specific three-body repulsion [50], and it is believed to be in the same universality class of the FQH state observed at filling $\nu = 5/2$ [51–53].

In the presence of properly designed external potentials, the ground state may also host a specific number of

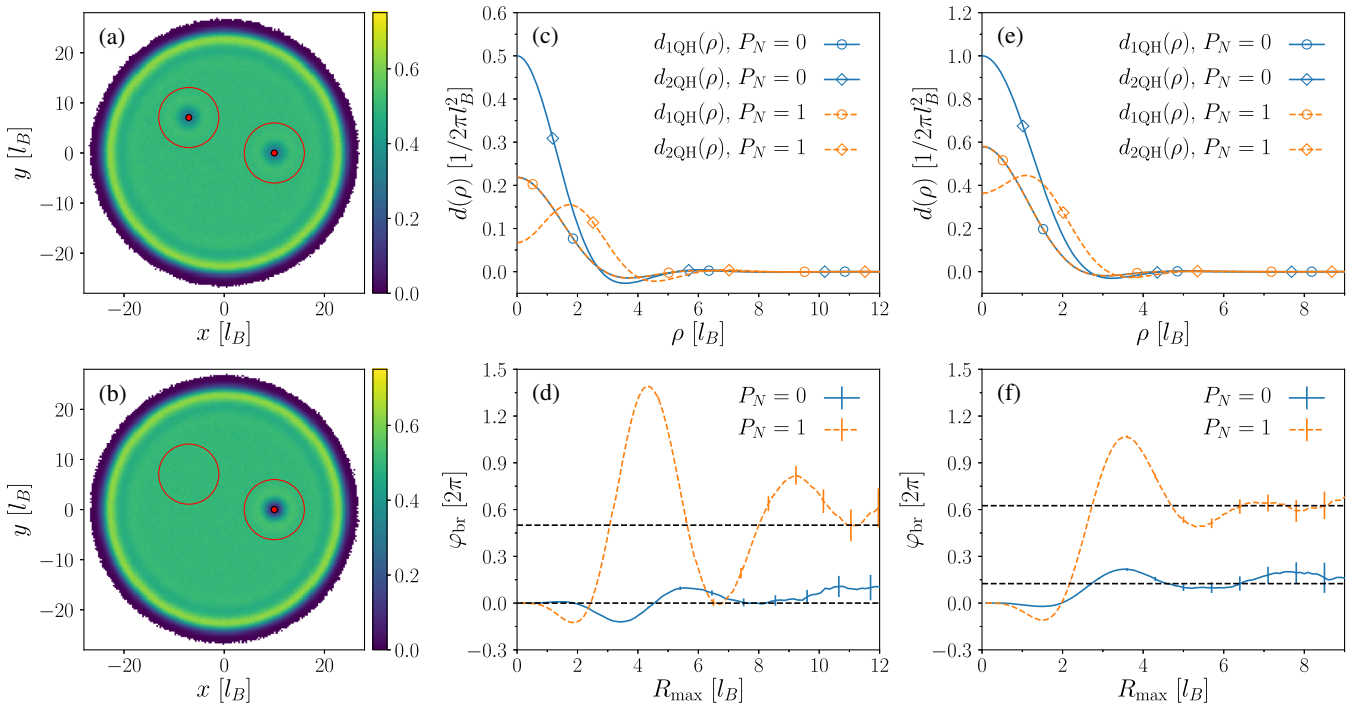

FIG. 2. (a) 2D density profile of the $N=150$ $M=2$ Moore-Read state with quasiholes at positions $\eta_1=10l_B$ and $\eta_2=10e^{i3\pi/2}l_B$ (red dots). (b) 2D density profile of the $N=150$ $M=2$ Moore-Read state with quasiholes at positions $\eta_1=\eta_2=10l_B$. Red circles give a pictorial representation of the regions A_1 and A_2 where the 2D densities depicted in (a) and (b) are different. (c) Radial profile of the density depletions caused by a single quasihole at $\eta_1=0$ (circles) and two quasiholes on top of each other at $\eta_1=\eta_2=0$ (diamonds), for even (blue solid lines) and odd (orange dashed lines) parity of N, at filling $\nu=1/M=1/2$. We consider $N=200$ or $N=199$. (d) Quasihole braiding phase evaluated with Eq. (13) as a function of the cutoff radius R_{max}, for both $P_N=0$ (blue solid line) and $P_N=1$ (orange dashed line) in the $M=2$ fermionic case. Black dashed lines denote the predictions for φ_{br} [see Eq. (9)]. [(e) and (f)] Same as (c) and (d) for the $M=1$ bosonic case.

localized anyonic excitations [34–36]. The quasihole (QH) excitations of the MR state obey non-Abelian statistics [8,12,20]. In particular, they are Ising anyons with an additional Abelian contribution to their statistical phase, and they can fuse in two different ways. For a given set of coordinates $(\eta_1,\ldots,\eta_{2n})$ of $2n$ such QHs, there is a 2^{n-1}-fold degenerate set of states [20].

In the following, we consider the case $2n=2$, for which the system is not degenerate. In this case, the MR wave function $\Psi^{2\mathrm{QH}}$ has the same form as in Eq. (7); yet the antisymmetric matrix W depends on the even or odd parity $P_N=0,\ 1$ of the particle number N. For $P_N=0$, it is $N\times N$ and reads

$$W_{ij}=\frac{(\eta_1-z_i)(\eta_2-z_j)+(i\leftrightarrow j)}{z_i-z_j}\qquad\forall\, i\neq j. \tag{8}$$

For $P_N=1$, on the other hand, W is a $(N+1)\times(N+1)$ matrix. The $N\times N$ upper-left block is defined as in Eq. (8), while the entries of the $(N+1)$th row (column) are equal to $+1$ (-1) [37].

The fusion channel of the two QHs depends on P_N [21]. As a consequence, the braiding of two MR QHs induces a phase φ_{br} that depends on P_N,

$$\frac{\varphi_{\mathrm{br}}}{2\pi}=\frac{1}{4M}-\frac{1}{8}+\frac{P_N}{2}. \tag{9}$$

The dependence of the braiding phase φ_{br} on P_N is thus a direct indication of the non-Abelian statistics of QHs, because it indicates that the two QHs are in different fusion channels when N is even or odd [12].

φ_{br} from the mean square radius.—As previously mentioned, for a 2π-rotation of the QHs, $\mathcal{B}$ is the identity matrix. For the nondegenerate MR state with two QHs, the unitary transformation $\mathcal{U}(T)$ associated with this process reduces to the phase factor $\mathcal{U}_B=e^{i\varphi_B}$, where $\varphi_B=2\pi\mathcal{L}/\hbar$ is the Berry phase. In this case, $\mathcal{L}$ is the expectation value of the angular-momentum operator over the initial state, $\langle\hat{L}_z\rangle$.

The Berry phase φ_B has a nontopological contribution, which can be interpreted as an Aharonov-Bohm phase [37]. Although this phase factor contains information on the QH fractional charge, we have to remove it to isolate the QH braiding phase φ_{br}. To this purpose we consider the difference between the Berry phases for two particular states [see Figs. 2(a) and 2(b)],

$$\frac{\varphi_{\mathrm{br}}}{2\pi}=\frac{1}{\hbar}[\langle\hat{L}_z\rangle_{|\eta_1|=|\eta_2|}-\langle\hat{L}_z\rangle_{\eta_1=\eta_2}]. \tag{10}$$

TABLE I. Quasihole braiding phase $\varphi_{\rm br}^{\rm MC}$ obtained numerically via Eq. (11) (third column, with the Monte Carlo statistical uncertainty) and its prediction $\varphi_{\rm br}$ in Eq. (9) (fourth column), for $M = 2$, 1 and for different parities P_N of the particle number $N = 150$ and $N = 149$. For the $|\eta_1| = |\eta_2|$ term in Eq. (11), we set $\eta_1 = -\eta_2$, which is the optimal configuration for a finite-size system. For the $M = 2$ ($M = 1$) case, $|\eta_1|/l_B$ is equal to 7.5 (6.5).

M	P_N	$\varphi_{\rm br}^{\rm MC}$ $[2\pi]$	$\varphi_{\rm br}$ $[2\pi]$
2 (fermions)	0	0.05 ± 0.06	0
	1	0.49 ± 0.07	0.5
1 (bosons)	0	0.13 ± 0.04	0.125
	1	0.59 ± 0.04	0.625

The expectation value $\langle \hat{L}_z \rangle_{|\eta_1|=|\eta_2|}$ is taken on a state with QHs sufficiently far from each other, at positions η_1 and η_2 such that $|\eta_1| = |\eta_2|$. On the other hand, $\langle \hat{L}_z \rangle_{\eta_1=\eta_2}$ is measured on the state with the two QHs on top of each other at $\eta_1 = \eta_2$ (for details, see Ref. [37]).

The mean angular momentum of a state in the LLL is related to its mean square radius, $\langle \hat{L}_z \rangle/\hbar + N = N\langle r^2 \rangle/2l_B^2$ [44,54]. This simplifies Eq. (10), which reads

$$\frac{\varphi_{\rm br}}{2\pi} = \frac{N}{2l_B^2}[\langle r^2 \rangle_{|\eta_1|=|\eta_2|} - \langle r^2 \rangle_{\eta_1=\eta_2}]. \tag{11}$$

Moreover, within the LLL approximation, the mean square radius of the cloud, and so $\varphi_{\rm br}$, can be measured after time-of-flight expansion [44,55].

To validate Eq. (11), we compute $\langle r^2 \rangle$ through the Monte Carlo technique [37]. Numerical results, reported in Table I for both $M = 2$ (fermionic case) and $M = 1$ (bosonic case) and for different parities P_N of the particle number N, are fully compatible with Eq. (9). This demonstrates that the existence of multiple fusion channels for the MR QHs can be experimentally probed without braiding them.

$\varphi_{\rm br}$ from the quasihole density depletions.—Although the protocol suggested in Eq. (11) is already close to the current experimental capabilities, it requires the ability to pin QHs with high precision and knowledge of the particle number. Moreover, $\varphi_{\rm br}$ is difficult to compute for large systems, since it is a $\mathcal{O}(1)$ number obtained as the difference between two $\mathcal{O}(N^2)$ quantities. However, Eq. (11) can be recast in a form that depends neither on N nor on the precise QH positions, as we prove in the following. Because of the incompressibility of the FQH states [7], the densities of the configurations under study only differ in the regions A_1 and A_2 surrounding the QHs [see red circles in Figs. 2(a) and 2(b)]. Therefore, the integrals in Eq. (11) can be restricted to A_1 and A_2,

$$\frac{\varphi_{\rm br}}{2\pi} = \frac{1}{2l_B^2}\int_{A_1,A_2} r^2[n_{|\eta_1|=|\eta_2|}(\vec{r}) - n_{\eta_1=\eta_2}(\vec{r})]d\vec{r}. \tag{12}$$

In these regions, the densities in Eq. (12) can be expressed in terms of the density depletions $d_{\rm 1QH}$ and $d_{\rm 2QH}$ caused by a single QH and two overlapping QHs [37]. This allows us to write the braiding phase as

$$\frac{\varphi_{\rm br}}{2\pi} = \frac{1}{2l_B^2}\int d\vec{\rho}\rho^2[d_{\rm 2QH}(\vec{\rho}) - 2d_{\rm 1QH}(\vec{\rho})], \tag{13}$$

in which $\vec{\rho}$ is the distance from a QH position, $d_{\rm 1QH}(\vec{\rho}) = n_B - n_{|\eta_1|=|\eta_2|}(\vec{\rho} + \eta_i)$ and $d_{\rm 2QH}(\vec{\rho}) = n_B - n_{\eta_1=\eta_2}(\vec{\rho} + \eta_i)$ are the aforementioned QH density depletions, with respect to the bulk density $n_B = 1/2\pi M l_B^2$ [see Figs. 2(c) and 2(e)]. The integration region must be large enough to ensure an appropriate decay of the density oscillations induced by the QHs. At the same time, a cutoff $\rho < R_{\rm max}$ is needed to avoid spurious contributions coming from the density deformations generated at the cloud boundaries. The numerical validation of Eq. (13) is shown in Figs. 2(d) and 2(f) for the different parities P_N, and for $M = 2$, 1. Residual deviations from the expected $\varphi_{\rm br}$ are due to finite-size effects.

Equation (13) constitutes an operative way to measure $\varphi_{\rm br}$, which depends only on local properties in the bulk region. As such, it is robust against edge modes, which are the typical low-energy excitations due to finite-temperature effects [33,56]. Moreover, since $d_{\rm 1QH}(\rho)$ does not depend on P_N [see Figs. 2(c) and 2(e)], all the information on the fusion channels is encoded in $d_{\rm 2QH}(\rho)$, which is completely different for even and odd values of N. Although this dependence on P_N was already known [36,39], the key result of our work is that the depletion profiles also contain quantitative information on the braiding phase. Note that this result holds for the QH excitations of any state in the LLL.

Experimental procedure.—While $d_{\rm 1QH}(\rho)$ can be indifferently measured in the ground state with either a single QH or two well-separated ones [34,35], the characterization of two overlapping QHs involves more subtleties: First, the state in Eq. (8) with overlapping QHs may not be the ground state in the presence of a given external potential. For instance, for odd parity P_N, having two QHs close to each other might cost more energy than just exciting a low-energy fermionic excitation at the boundary [34,49,57]. Furthermore, the presence of these fermionic edge modes may modify the relation between the QHs fusion channel and the particle number parity P_N (see footnote [33] in Ref. [35]).

We thus propose to proceed as follows for the measurement of $d_{\rm 2QH}(\rho)$: two QHs are created far apart, by cooling the system in the presence of pinning potentials. The two QHs are then slowly brought closer and fused [37]. According to the general theory of topological quantum computation [12,58], the fusion channel cannot change during this process, so the system is adiabatically transported into the (possibly metastable) desired state, where

the depletion profile $d_{2QH}(\rho)$ is measured. Note that unless special care is taken, we can argue that in an actual experiment the QH fusion channel is randomly chosen at each repetition [37]. Nonetheless, the non-Abelian statistics of the QHs are still visible in the bipeaked probability for φ_{br}. A rigorous proof of this statement requires numerical experiments based on a model Hamiltonian and a particular cooling mechanism; we leave it for a future study.

Conclusions and outlook.—In this work, we presented a scheme to assess the statistical properties of anyonic excitations that does not rely on any kind of interference. Our protocol is based on a mathematical link between statistics and angular-momentum measurements, derived by considering rigid rotations of the anyons. This relation further simplifies for states in the LLL, where anyonic statistics is encoded in the density profile. Having access to the anyonic statistics without performing any interference scheme is remarkable in itself; moreover, relating statistics to density measurements makes our protocol readily applicable to state-of-the-art experiments with ultracold atoms [30] and photons [32].

Beyond the identification of the Moore-Read fusion channels, on which our scheme has been validated, the study of the two-anyons case opens several other perspectives. For example, our method can be employed to distinguish the Moore-Read and anti-Pfaffian states, whose quasiholes have different Abelian contributions to the braiding phase [59–64]. Moreover, it gives access to a key property in topological quantum computation [12,58], namely, the dependence of the braiding phase on the distance between the anyons [17].

Our method can also be useful for theoretical studies of states supporting anyons of unknown type. When one can compute the matrix elements of the angular-momentum and rotation operators in the ground-state manifold, our scheme gives access to all contributions to the time-evolution operator, for any rigid rotation of the anyons. We stress that in the case of non-Abelian anyons rigid rotations are sufficient to induce nontrivial mixing of the ground states [12], although only a subset of the possible anyonic exchanges is accessible in this way [37]. Therefore, we envision the possibility of a more precise theoretical characterization of the anyons, beyond the present identification of fusion channels.

Natural extensions of our analysis include other states in the LLL—like the Read-Rezayi state [11]—or the p-wave superconductor, closely related to the Moore-Read state [9]. An exciting question is whether the link between the anyonic statistics and the system density remains valid also for lattice systems [18,65–68]; this is the subject of ongoing study [69].

This work was supported by the EU-FET Proactive grant AQuS, Grant No. 640800, and by the Autonomous Province of Trento, partially through the project "On silicon chip quantum optics for quantum computing and secure communications" ("SiQuro"). I. C. also thanks financial support from the European Union H2020-FETFLAG-2018-2020 grant "PhoQuS", Grant No. 820392. Stimulating discussions with P. Bonderson, M. Fremling, M. O. Goerbig, V. Gurarie, C. Nayak, N. Regnault, M. Rizzi, S. H. Simon, J. K. Slingerland, and R. O. Umucalılar are warmly acknowledged.

[1] F. Wilczek, Quantum Mechanics of Fractional-Spin Particles, Phys. Rev. Lett. **49**, 957 (1982).
[2] B. I. Halperin, Statistics of Quasiparticles and the Hierarchy of Fractional Quantized Hall States, Phys. Rev. Lett. **52**, 1583 (1984).
[3] D. Arovas, J. R. Schrieffer, and F. Wilczek, Fractional Statistics and the Quantum Hall Effect, Phys. Rev. Lett. **53**, 722 (1984).
[4] J. M. Leinaas and J. Myrheim, On the theory of identical particles, Il Nuovo Cimento B **37**, 1 (1977).
[5] Y.-S. Wu, General Theory for Quantum Statistics in Two Dimensions, Phys. Rev. Lett. **52**, 2103 (1984).
[6] January Special Issue 2008, edited by F. Wilczek [Anyons and the quantum Hall effect–A pedagogical review, Ann. Phys. (Amsterdam) **323**, 204 (2008)].
[7] D. Tong, Lectures on the quantum Hall effect, arXiv: 1606.06687.
[8] G. Moore and N. Read, Nonabelions in the fractional quantum Hall effect, Nucl. Phys. **B360**, 362 (1991).
[9] N. Read and D. Green, Paired states of fermions in two dimensions with breaking of parity and time-reversal symmetries and the fractional quantum Hall effect, Phys. Rev. B **61**, 10267 (2000).
[10] D. A. Ivanov, Non-Abelian Statistics of Half-Quantum Vortices in p-Wave Superconductors, Phys. Rev. Lett. **86**, 268 (2001).
[11] N. Read and E. Rezayi, Beyond paired quantum Hall states: Parafermions and incompressible states in the first excited Landau level, Phys. Rev. B **59**, 8084 (1999).
[12] C. Nayak, S. H. Simon, A. Stern, M. Freedman, and S. Das Sarma, non-Abelian anyons and topological quantum computation, Rev. Mod. Phys. **80**, 1083 (2008).
[13] R. L. Willett, L. N. Pfeiffer, and K. W. West, Measurement of filling factor $5/2$ quasiparticle interference with observation of charge e/4 and e/2 period oscillations, Proc. Natl. Acad. Sci. U.S.A. **106**, 8853 (2009).
[14] V. Mourik, K. Zuo, S. M. Frolov, S. R. Plissard, E. P. A. M. Bakkers, and L. P. Kouwenhoven, Signatures of Majorana fermions in hybrid superconductor-semiconductor nanowire devices, Science **336**, 1003 (2012).
[15] B. Paredes, P. Fedichev, J. I. Cirac, and P. Zoller, $\frac{1}{2}$-Anyons in Small Atomic Bose-Einstein Condensates, Phys. Rev. Lett. **87**, 010402 (2001).
[16] Y. Tserkovnyak and S. H. Simon, Monte Carlo Evaluation of non-Abelian Statistics, Phys. Rev. Lett. **90**, 016802 (2003).
[17] M. Baraban, G. Zikos, N. Bonesteel, and S. H. Simon, Numerical Analysis of Quasiholes of the Moore-Read Wave Function, Phys. Rev. Lett. **103**, 076801 (2009).

[18] Y.-L. Wu, B. Estienne, N. Regnault, and B. A. Bernevig, Braiding non-Abelian Quasiholes in Fractional Quantum Hall States, Phys. Rev. Lett. **113**, 116801 (2014).

[19] A. E. B. Nielsen, Anyon braiding in semianalytical fractional quantum Hall lattice models, Phys. Rev. B **91**, 041106 (R) (2015).

[20] C. Nayak and F. Wilczek, $2n$-quasihole states realize 2^{n-1}-dimensional spinor braiding statistics in paired quantum Hall states, Nucl. Phys. **B479**, 529 (1996).

[21] P. Bonderson, V. Gurarie, and C. Nayak, Plasma analogy and non-Abelian statistics for Ising-type quantum Hall states, Phys. Rev. B **83**, 075303 (2011).

[22] B. I. Halperin, A. Stern, I. Neder, and B. Rosenow, Theory of the Fabry-Pérot quantum Hall interferometer, Phys. Rev. B **83**, 155440 (2011).

[23] G. Campagnano, O. Zilberberg, I. V. Gornyi, D. E. Feldman, A. C. Potter, and Y. Gefen, Hanbury Brown–Twiss Interference of Anyons, Phys. Rev. Lett. **109**, 106802 (2012).

[24] S. Das Sarma, M. Freedman, and C. Nayak, Topologically Protected Qubits from a Possible non-Abelian Fractional Quantum Hall State, Phys. Rev. Lett. **94**, 166802 (2005).

[25] A. Stern and B. I. Halperin, Proposed Experiments to Probe the non-Abelian $\nu = 5/2$ Quantum Hall State, Phys. Rev. Lett. **96**, 016802 (2006).

[26] P. Bonderson, A. Kitaev, and K. Shtengel, Detecting non-Abelian Statistics in the $\nu = 5/2$ Fractional Quantum Hall State, Phys. Rev. Lett. **96**, 016803 (2006).

[27] F. E. Camino, W. Zhou, and V. J. Goldman, Realization of a Laughlin quasiparticle interferometer: Observation of fractional statistics, Phys. Rev. B **72**, 075342 (2005).

[28] B. Rosenow and B. I. Halperin, Influence of Interactions on Flux and Back-Gate Period of Quantum Hall Interferometers, Phys. Rev. Lett. **98**, 106801 (2007).

[29] L. Pitaevskii and S. Stringari, *Bose-Einstein Condensation and Superfluidity* (Oxford University Press, Oxford, 2016).

[30] N. R. Cooper, J. Dalibard, and I. B. Spielman, Topological bands for ultracold atoms, Rev. Mod. Phys. **91**, 015005 (2019).

[31] I. Carusotto and C. Ciuti, Quantum fluids of light, Rev. Mod. Phys. **85**, 299 (2013).

[32] T. Ozawa, H. M. Price, A. Amo, N. Goldman, M. Hafezi, L. Lu, M. C. Rechtsman, D. Schuster, J. Simon, O. Zilberberg, and I. Carusotto, Topological photonics, Rev. Mod. Phys. **91**, 015006 (2019).

[33] E. Macaluso and I. Carusotto, Ring-shaped fractional quantum Hall liquids with hard-wall potentials, Phys. Rev. A **98**, 013605 (2018).

[34] X. Wan, K. Yang, and E. H. Rezayi, Edge Excitations and non-Abelian Statistics in the Moore-Read State: A Numerical Study in the Presence of Coulomb Interaction and Edge Confinement, Phys. Rev. Lett. **97**, 256804 (2006).

[35] X. Wan, Z.-X. Hu, E. H. Rezayi, and K. Yang, Fractional quantum Hall effect at $\nu = 5/2$: Ground states, non-Abelian quasiholes, and edge modes in a microscopic model, Phys. Rev. B **77**, 165316 (2008).

[36] E. Prodan and F. D. M. Haldane, Mapping the braiding properties of the Moore-Read state, Phys. Rev. B **80**, 115121 (2009).

[37] See Supplemental Material at http://link.aps.org/supplemental/10.1103/PhysRevLett.123.266801, which includes Refs. [8,20,21,34,35,38–49], for an alternative derivation of Eqs. (5) and (6), for the explicit calculation of the Aharonov-Bohm contribution to $\langle \hat{L}_z \rangle$, for a more detailed discussion about possible experimental issues, and for the extension of the rigid-rotation formalism to the case of four Moore-Read quasiholes.

[38] L. E. Picasso, *Lectures in Quantum Mechanics* (Springer International Publishing, Berlin, 2016).

[39] M. S. Baraban, Low energy excitations in quantum condensates, Ph.D. thesis, 2010.

[40] N. Metropolis, A. W. Rosenbluth, M. N. Rosenbluth, A. H. Teller, and E. Teller, Equation of state calculations by fast computing machines, J. Chem. Phys. **21**, 1087 (1953).

[41] W. Krauth, *Statistical Mechanics: Algorithms and Computations* (Oxford University Press, Oxford, 2006).

[42] R. Morf and B. I. Halperin, Monte Carlo evaluation of trial wave functions for the fractional quantized Hall effect: Disk geometry, Phys. Rev. B **33**, 2221 (1986).

[43] H. Kjønsbergand J. Myrheim, Numerical study of charge and statistics of Laughlin quasiparticles, Int. J. Mod. Phys. A **14**, 537 (1999).

[44] R. O. Umucalılar, E. Macaluso, T. Comparin, and I. Carusotto, Time-of-Flight Measurements as a Possible Method to Observe Anyonic Statistics, Phys. Rev. Lett. **120**, 230403 (2018).

[45] M. Born and V. Fock, Beweis des Adiabatensatzes, Z. Phys. **51**, 165 (1928).

[46] G. Rigolin and G. Ortiz, Adiabatic theorem for quantum systems with spectral degeneracy, Phys. Rev. A **85**, 062111 (2012).

[47] F. Wilczek and A. Zee, Appearance of Gauge Structure in Simple Dynamical Systems, Phys. Rev. Lett. **52**, 2111 (1984).

[48] Y. Aharonov and D. Bohm, Significance of electromagnetic potentials in the quantum theory, Phys. Rev. **115**, 485 (1959).

[49] X.-G. Wen, Topological orders and edge excitations in fractional quantum Hall states, Adv. Phys. **44**, 405 (1995).

[50] M. Greiter, X.-G. Wen, and F. Wilczek, Paired Hall State at Half Filling, Phys. Rev. Lett. **66**, 3205 (1991).

[51] M. Greiter, X.-G. Wen, and F. Wilczek, Paired Hall states, Nucl. Phys. **B374**, 567 (1992).

[52] R. H. Morf, Transition from Quantum Hall to Compressible States in the Second Landau Level: New Light on the $\nu = 5/2$ Enigma, Phys. Rev. Lett. **80**, 1505 (1998).

[53] E. H. Rezayi and F. D. M. Haldane, Incompressible Paired Hall State, Stripe Order, and the Composite Fermion Liquid Phase in Half-Filled Landau Levels, Phys. Rev. Lett. **84**, 4685 (2000).

[54] T.-L. Ho and E. J. Mueller, Rotating Spin-1 Bose Clusters, Phys. Rev. Lett. **89**, 050401 (2002).

[55] N. Read and N. R. Cooper, Free expansion of lowest-Landau-level states of trapped atoms: A wave-function microscope, Phys. Rev. A **68**, 035601 (2003).

[56] E. Macaluso and I. Carusotto, Hard-wall confinement of a fractional quantum Hall liquid, Phys. Rev. A **96**, 043607 (2017).

[57] M. Milovanović and N. Read, Edge excitations of paired fractional quantum Hall states, Phys. Rev. B **53**, 13559 (1996).

[58] A. Y. Kitaev, Fault-tolerant quantum computation by anyons, Ann. Phys. (Amsterdam) **303**, 2 (2003).

[59] M. Levin, B. I. Halperin, and B. Rosenow, Particle-Hole Symmetry and the Pfaffian State, Phys. Rev. Lett. **99**, 236806 (2007).

[60] S.-S. Lee, S. Ryu, C. Nayak, and M. P. A. Fisher, Particle-Hole Symmetry and the $\nu = \frac{5}{2}$ Quantum Hall State, Phys. Rev. Lett. **99**, 236807 (2007).

[61] D. T. Son, Is the Composite Fermion a Dirac Particle?, Phys. Rev. X **5**, 031027 (2015).

[62] S. H. Simon, Interpretation of thermal conductance of the $\nu = \mathbf{5/2}$ edge, Phys. Rev. B **97**, 121406(R) (2018).

[63] D. E. Feldman, Comment on "Interpretation of thermal conductance of the $\nu = 5/2$ edge", Phys. Rev. B **98**, 167401 (2018).

[64] S. H. Simon, Reply to "Comment on 'Interpretation of thermal conductance of the $\nu = 5/2$ edge'", Phys. Rev. B **98**, 167402 (2018).

[65] M. Hafezi, A. S. Sørensen, E. Demler, and M. D. Lukin, Fractional quantum Hall effect in optical lattices, Phys. Rev. A **76**, 023613 (2007).

[66] L. Mazza, M. Rizzi, M. Lewenstein, and J. I. Cirac, Emerging bosons with three-body interactions from spin-1 atoms in optical lattices, Phys. Rev. A **82**, 043629 (2010).

[67] N. Regnault and B. A. Bernevig, Fractional Chern Insulator, Phys. Rev. X **1**, 021014 (2011).

[68] M. Hafezi, P. Adhikari, and J. M. Taylor, Engineering three-body interaction and Pfaffian states in circuit QED systems, Phys. Rev. B **90**, 060503(R) (2014).

[69] E. Macaluso, T. Comparin, R. O. Umucalılar, M. Gerster, S. Montangero, M. Rizzi, and I. Carusotto, Charge and statistics of lattice quasiholes from density measurements: A Tree Tensor Network study, arXiv:1910.05222.